Optics Letters

# Self-referenced frequency combs using high-efficiency silicon-nitride waveguides

David R. Carlson,[1,*] Daniel D. Hickstein,[1] Alex Lind,[1,2] Stefan Droste,[3] Daron Westly,[4] Nima Nader,[3] Ian Coddington,[3] Nathan R. Newbury,[3] Kartik Srinivasan,[4] Scott A. Diddams,[1,2] and Scott B. Papp[1,2]

[1]Time and Frequency Division, National Institute of Standards and Technology, 325 Broadway, Boulder, Colorado 80305, USA
[2]Department of Physics, University of Colorado, 2000 Colorado Ave., Boulder, Colorado 80309, USA
[3]Applied Physics Division, National Institute of Standards and Technology, 325 Broadway, Boulder, Colorado 80305, USA
[4]Center for Nanoscale Science and Technology, National Institute of Standards and Technology, 100 Bureau Drive, Gaithersburg, Maryland 20899, USA
*Corresponding author: david.carlson@nist.gov

Received 13 April 2017; revised 14 May 2017; accepted 17 May 2017; posted 19 May 2017 (Doc. ID 292633); published 12 June 2017

**We utilize silicon-nitride waveguides to self-reference a telecom-wavelength fiber frequency comb through supercontinuum generation, using 11.3 mW of optical power incident on the chip. This is approximately 10 times lower than conventional approaches using nonlinear fibers and is enabled by low-loss (<2 dB) input coupling and the high nonlinearity of silicon nitride, which can provide two octaves of spectral broadening with incident energies of only 110 pJ. Following supercontinuum generation, self-referencing is accomplished by mixing 780-nm dispersive-wave light with the frequency-doubled output of the fiber laser. In addition, at higher optical powers, we demonstrate $f$-to-3$f$ self-referencing directly from the waveguide output by the interference of simultaneous supercontinuum and third harmonic generation, without the use of an external doubling crystal or interferometer. These hybrid comb systems combine the performance of fiber-laser frequency combs with the high nonlinearity and compactness of photonic waveguides, and should lead to low-cost, fully stabilized frequency combs for portable and space-borne applications.**

***OCIS codes:*** (190.4390) Nonlinear optics, integrated optics; (320.6629) Supercontinuum generation; (320.7110) Ultrafast nonlinear optics.

https://doi.org/10.1364/OL.42.002314

Chip-integrated photonic waveguides, due to their high spatial light confinement and strong nonlinear response, are ideally suited for performing nonlinear optics with femtosecond laser pulses. In particular, waveguide-based supercontinuum generation (SCG) using mode-locked laser frequency combs can produce broadband comb spectra spanning up to several hundred terahertz in a variety of different material platforms including silica [1,2], silicon-on-insulator [3,4], AlGaAs [5], chalcogenide glasses [6], aluminum nitride (AlN) [7], and silicon nitride ($Si_3N_4$, henceforth SiN) [8–11]. In addition to possessing high nonlinearity, the SiN platform is especially attractive for many applications because of its compatibility with standard silicon fabrication techniques and for having a broad transparency window extending from the visible to the mid-infrared. For example, these characteristics have recently allowed SiN waveguides to produce tailored two-octave output spectra suitable for precision frequency metrology [12].

In addition to generating broad bandwidth, SiN offers an attractive way to generate the comb offset $f_0$. Offset-frequency stabilization is most commonly accomplished using a self-referencing technique called $f$-to-2$f$ interferometry [13] that, for any fiber laser system, requires spectral broadening in a nonlinear fiber. Such nonlinear fibers require high peak powers to generate sufficient bandwidth, and consequently optical amplifiers, or high-power pump lasers are often needed to provide enough pulse energy prior to broadening. On the other hand, the high nonlinearity and tight confinement of SiN allows much lower energies to be used for $f$-to-2$f$ broadening while additionally having a more compact form-factor [14,15]. Furthermore, SiN can support spectral broadening to twice the pump frequency to allow decoupling of the nonlinear broadening and frequency-doubling processes for reduced sensitivity to external perturbations [2,12].

Offset-frequency stabilization of 1550 nm telecom-wavelength combs using nonlinear waveguides is of particular interest because these comb systems are well-developed, have low-cost components readily available, and are successfully used in many diverse fields. However, field-portable, space-borne, and integrated applications for these combs have very tight power and cost budgets. In such cases, a simple and low-power self-referencing solution is required [16–18]. Waveguide-broadened combs operating in the low-pulse-energy regime are also important as they offer a path toward the stabilization of high repetition rate electro-optic combs [19] and fully chip-integrated microresonator combs [20].

In this Letter, we present two approaches to self-referencing frequency combs with stoichiometric SiN waveguides that

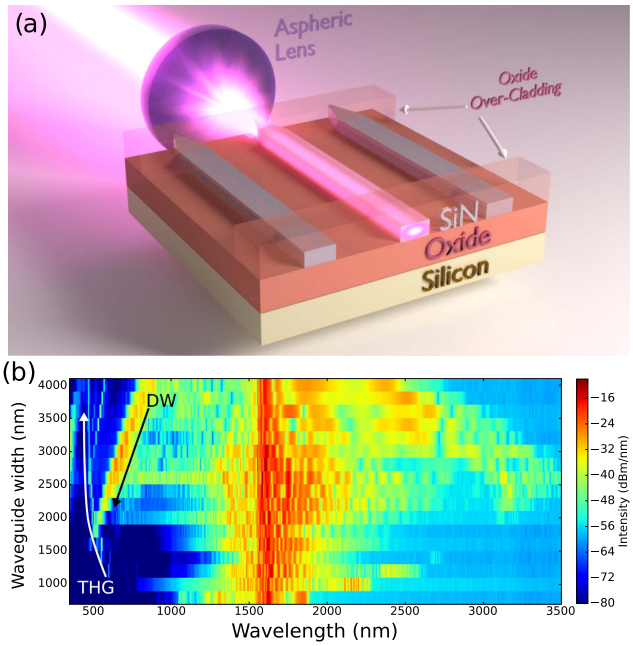


**Fig. 1.** (a) Air-clad silicon nitride (SiN) waveguides with 700 nm thickness, 1 cm length, and varying widths. An inverse taper geometry at the input facet yields coupling loss less than 2 dB, while an oxide over-cladding at both input and output facets improves mode matching with free space optics. (b) Supercontinuum spectra from SiN waveguides of different waveguide widths pumped with a 100 MHz repetition rate, 1550 nm fiber-laser frequency comb (DW, dispersive wave; THG, third-harmonic generation). For these spectra, the pulse energy was 1 nJ, the full-width at half-maximum pulse duration was 80 fs, and the total average power was 100 mW. Increasing the pulse energy up to 2 nJ does not significantly alter the spectrum but can increase the conversion efficiency to the dispersive wave.

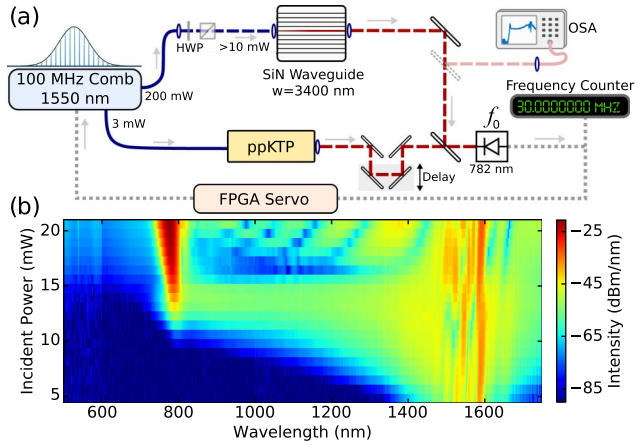


**Fig. 2.** (a) Schematic of low-power self-referencing scheme (fiber path: solid lines, free-space: dashed lines, electrical path: dotted gray lines, HWP: half-wave plate, PBS: polarizing beam-splitter, OSA: optical spectrum analyzer). A turn-key fiber-laser frequency comb is coupled into a 3400 nm width silicon nitride waveguide. The waveguide output is collected with a 0.85 NA microscope objective and overlapped with doubled pump light from a periodically-poled potassium titanyl phosphate (ppKTP) waveguide to obtain an $f_0$ signal after photodetection. The offset frequency is locked using a digital FPGA-based servo loop by feeding back to the fiber laser pump current. A flipper mirror can be used to divert the waveguide output light to a multimode fiber for recording the optical spectrum as a function of average incident laser power as shown in (b). A dispersive wave at 775 nm is observed with at least 10 mW of incident power.

demonstrate the flexibility of this chip-integrated approach. First, we demonstrate a waveguide design with improved input-coupling that enables $f_0$ stabilization with less than 15 mW total power (150 pJ of pulse energy) including for second-harmonic generation, a level attainable directly from fiber laser oscillators. Second, we show that SiN waveguides pumped with higher powers can achieve simultaneous SCG and third-harmonic generation (THG) and enable $f$-to-$3f$ self-referencing directly from the waveguide. The resulting $2f_0$ beat frequency is used for comb-offset stabilization without the use of an external interferometer or a nonlinear doubling medium—greatly simplifying the standard $f$-to-$2f$ technique and reducing the overall cost of the system.

The 1 cm long chip-integrated waveguides used in this work have an air-clad ridge geometry [Fig. 1(a)] and are made of 700 nm thickness low pressure chemical vapor deposition (LPCVD) stoichiometric SiN. The waveguide pattern is written to the chip using electron-beam lithography and includes inverse tapers at the input facet to improve optical coupling [21]. Though several techniques have been demonstrated to offer very high efficiency fiber-to-waveguide coupling [22–24], free-space coupling is used here for convenience. An input coupling loss of less than 2 dB is achieved using an aspheric lens with a design wavelength of 1550 nm and numerical aperture (NA) of 0.6. In addition to the inverse taper region that adiabatically expands the mode, there is an oxide over-cladding near the edges of the chip to improve the mode symmetry and overlap with the incident beam [25]. However, the output of the waveguide is not tapered to achieve consistent output coupling across the spectrum and to avoid additional absorption of the long-wavelength spectral components in the fully oxide-clad region [Fig. 1(a)].

The frequency comb source is an amplified 1550-nm mode-locked all-polarization-maintaining fiber laser producing 80 fs FWHM $\text{sech}^2$ pulses at an average power of 200 mW ($f_r = 100$ MHz) [26]. For these tests, its output is attenuated using a half-wave-plate and polarizing beam-splitter before coupling to the waveguide. We operate the amplifier at higher power than is necessary for SCG in the waveguide to maintain optimal pulse compression. However, such short pulses could be obtained directly from an appropriately configured laser oscillator without an external amplifier [27,28].

The SCG spectrum for an incident pulse energy of 1 nJ is shown in Fig. 1(b) as a function of waveguide width. Light covering more than two octaves of bandwidth is generated from approximately 500 nm to beyond 3 μm and is similar to the SiN spectra recently reported in [29]. For self-referencing, the two relevant features of the supercontinuum are the short-wavelength dispersive wave and third-harmonic generated light, as discussed in the following sections.

For $f$-to-$2f$ interferometry, we exploit the dispersive wave in the 782 nm spectral region that is generated by the 3400 nm wide waveguide, as shown in Fig. 1(b). This light can then be heterodyned against doubled light from the 1550-nm fiber-laser pulses to generate the offset frequency. In contrast to the

traditional approach in highly nonlinear fiber of achieving an octave-spanning spectrum and then mixing doubled 2 μm light with fundamental 1 μm light, in this method we have effectively decoupled the SCG from the frequency doubling. This allows for more relaxed requirements on the SCG and reduces the sensitivity to spectral power fluctuations.

Detection and subsequent stabilization of the comb offset frequency at 782 nm is accomplished using the schematic setup shown in Fig. 2(a). The SCG spectra obtained from the 3400 nm width waveguide at low incident average powers is shown in Fig. 2(b). The sharp onset of dispersive wave generation at 10 mW incident power indicates the threshold for soliton fission [30]. An $f$-to-$2f$ interferometer combines this dispersive wave with doubled light generated by diverting a small amount (3 mW) of the comb power to a periodically-poled fiber-coupled potassium titanyl phosphate (ppKTP) waveguide. The detected $f_0$ beat note is shown in Fig. 3(a) for different incident powers to the waveguide. A digital field-programmable gate array (FPGA) servo loop filter digitizes and electronically filters the offset frequency signal before applying a correction signal to the fiber laser's pump with approximately 60 kHz bandwidth [26].

For an electronic out-of-loop verification that the comb-offset lock is performing as expected, we count the locked offset frequency with a standard high-resolution commercial frequency counter (Λ-type). This counter requires a greater than 25 dB signal-to-noise ratio (SNR) in a 1 MHz resolution bandwidth (RBW), which is achieved here for incident laser power onto the waveguide as low as 11.3 mW. Figure 3(c) shows the counter record of the stabilized in-loop offset frequency at 30 MHz for 7.5 h of continuous operation. No cycle slips are observed within this period, indicating a robust phase lock is achieved. At an averaging time of $\tau = 1$ s, the in-loop frequency instability is $1 \times 10^{-17}$ and averages down continuously over the duration of the measurement. The integrated phase noise of the locked offset frequency is 6 rad [from 1 Hz to 4 MHz, see typical phase noise in Fig. 3(d)], and is set by the noise properties of this soliton laser design and feedback bandwidth, and not the $f$-to-$2f$ detection [26]. To the best of our knowledge, this is the lowest total average power used to self-reference a frequency comb through nonlinear broadening.

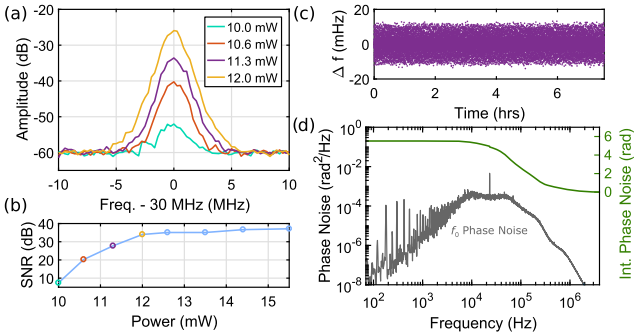


**Fig. 3.** (a) Locked offset-frequency and (b) corresponding SNR as a function of incident laser power at 1 MHz RBW. (c) In-loop frequency deviation $\Delta f = f_0 - 30$ MHz as recorded by an external frequency counter (1 s gate time) while $f_0$ is locked using 11.3 mW incident optical power. The comb is locked without cycle slips for the full 7.5 h acquisition. (d) Typical phase noise spectrum of locked $f_0$ beat note. The green curve shows the integrated phase noise (right axis).

For applications where simplicity takes priority over optical power consumption, we demonstrate an alternative self-referencing scheme using SiN waveguides that eliminates the external doubling crystal and the interferometer. This technique is similar to the recently reported $f$-to-$2f$ stabilization directly from the output of aluminum nitride (AlN) waveguides, which exploited the simultaneous presence of both second-order $\chi^{(2)}$ and third-order $\chi^{(3)}$ nonlinearities [7]. However, because SiN is centrosymmetric and thus only supports $\chi^{(3)}$, only third harmonic light can be generated, and we instead require supercontinuum broadening to $3f$. In this case, the resulting beat note from the interference between comb modes $3\nu_n$ and $\nu_{3n}$ due to simultaneous THG and SCG, respectively, occurs at frequency

$$3\nu_n - \nu_{3n} = 3(nf_r + f_0) - (3nf_r + f_0) = 2f_0. \quad \textbf{(1)}$$

The spectra displayed in Fig. 1(b) show that for a waveguide width of 1800 nm, the THG peak and dispersive wave intersect near 520 nm. In this region it is possible to both observe and lock the $2f_0$ beat frequency from Eq. (1). A schematic of the detection scheme and spectrum from the waveguide are shown in Fig. 4. The collimated waveguide output is spectrally filtered using a prism and then spatially filtered by a small-area avalanche-photodetector to find the highest degree of mode overlap.

The wavelength of the third-harmonic peak is determined by the phase-matching conditions to higher-order waveguide modes. As the waveguide dimensions are modified, the precise wavelength and number of modes that meet these conditions can change, hence the bifurcation in Fig. 1(b) for widths larger than 2800 nm. Also, although it is not readily visible in the optical spectrum, there are two different phase-matched THG modes in the photodetected region that can contribute to the $f$-to-$3f$ signal. Unfortunately, these higher order modes ($TE_{02}$ and $TE_{41}$, see Fig. 5) only exhibit very small spatial overlap (i.e., heterodyne mixing efficiency) with the fundamental mode in both the near- and far-field, limiting the achievable

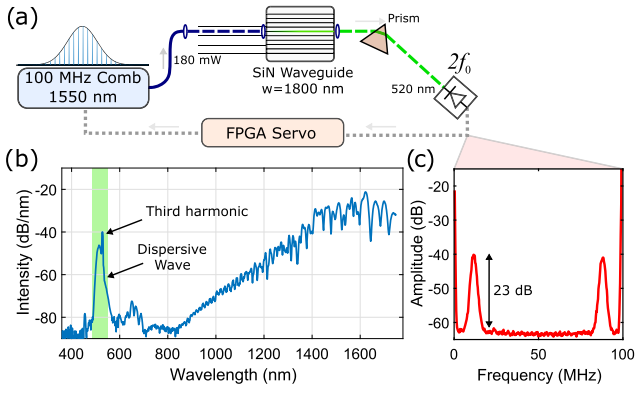


**Fig. 4.** (a) Schematic for $f$-to-$3f$ self-referencing (fiber path: solid lines, free-space: dashed lines, electrical path: dotted gray lines). The waveguide output is collimated and spectrally resolved using a prism before illuminating a photodetector. (b) SCG spectrum of the 1800-nm wide waveguide from Fig. 1 showing overlapped third-harmonic and dispersive wave contributions. The highlighted region is photodetected to obtain a beat frequency for $f$-to-$3f$ self-referencing. (c) RF signal at $2f_0$, obtained directly from the SiN waveguide output. The beat, with a signal-to-noise ratio of 23 dB at 1 MHz RBW, is suitable for locking using a feedback servo.

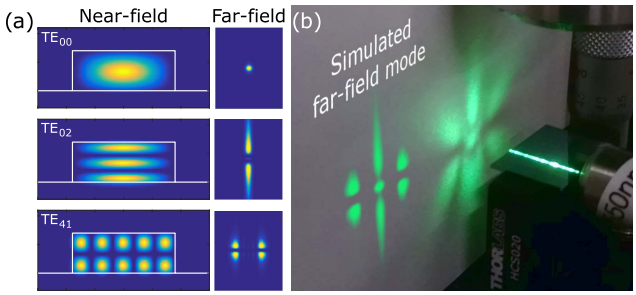


**Fig. 5.** (a) Simulated near-field and far-field intensity profiles at a wavelength of 520 nm for the modes of the 1800-nm width waveguide contributing to $f$-to-$3f$ self-referencing. The calculations were performed using the *wgmodes* mode solver [32]. (b) Experimental (right) and simulated (left) output mode obtained from a rectilinear projection of the combined modes in (a). Poor mode overlap limits the achievable beat note SNR.

SNR. Temporal overlap between the $f$ and $3f$ spectral components is also a concern because the narrow-bandwidth spectrum of the third harmonic leads to a longer pulse, and the waveguide modal dispersion can lead to temporal walk-off. Nevertheless, the digital FPGA servo used in the system is able to lock to the optimized 23 dB SNR $2f_0$ signal with approximately twice the integrated phase noise as in the low-power $f_0$ stabilization scheme, as expected from Eq. (1). However, due to insufficient SNR, it is not possible to verify this stabilization with our external frequency counter. In the future, an on-chip mode converter [31] could be used to isolate a single third-harmonic mode and achieve optimal spatial and temporal overlap for increasing the SNR of the $2f_0$ beat.

The two self-referencing techniques described in this work highlight the flexibility of the SiN material platform for supporting frequency comb systems. The low power consumption and experimental simplicity that are achievable with photonic integration will enable the widespread use of combs outside of the laboratory in applications ranging from fieldable dual-comb spectroscopy systems to space-based optical clocks, and to remote sensing.

**Funding.** Air Force Office of Scientific Research (AFOSR) (FA9550-16-1-0016); Defense Advanced Research Projects Agency (DARPA); National Aeronautics and Space Administration (NASA); National Institute of Standards and Technology (NIST); National Research Council (NRC).

**Acknowledgment.** This work is a contribution of the U.S. government and is not subject to copyright.

## REFERENCES

1. D. Y. Oh, D. Sell, H. Lee, K. Y. Yang, S. A. Diddams, and K. J. Vahala, Opt. Lett. **39**, 1046 (2014).
2. D. Y. Oh, K. Y. Yang, C. Fredrick, G. Ycas, S. A. Diddams, and K. J. Vahala, Nat. Commun. **8**, 13922 (2017).
3. I.-W. Hsieh, X. Chen, X. Liu, J. I. Dadap, N. C. Panoiu, C.-Y. Chou, F. Xia, W. M. Green, Y. A. Vlasov, and R. M. Osgood, Opt. Express **15**, 15242 (2007).
4. B. Kuyken, T. Ideguchi, S. Holzner, M. Yan, T. W. Hänsch, J. Van Campenhout, P. Verheyen, S. Coen, F. Leo, R. Baets, G. Roelkens, and N. Picqué, Nat. Commun. **6**, 6310 (2015).
5. K. Dolgaleva, W. C. Ng, L. Qian, J. S. Aitchison, M. C. Camasta, and M. Sorel, Opt. Lett. **35**, 4093 (2010).
6. B. J. Eggleton, B. Luther-Davies, and K. Richardson, Nat. Photonics **5**, 141 (2011).
7. D. Hickstein, H. Jung, D. R. Carlson, A. Lind, I. Coddington, K. Srinivasan, G. Ycas, D. Cole, A. Kowligy, C. Frederick, S. Droste, E. Lamb, N. Newbury, H. Tang, S. Diddams, and S. Papp, "Ultrabroadband supercontinuum generation and frequency-comb stabilization using on-chip waveguides with both cubic and quadratic nonlinearities," arXiv:1704.03908 (2017).
8. R. Halir, Y. Okawachi, J. S. Levy, M. A. Foster, M. Lipson, and A. L. Gaeta, Opt. Lett. **37**, 1685 (2012).
9. J. M. Chavez Boggio, D. Bodenmüller, T. Fremberg, R. Haynes, M. M. Roth, R. Eisermann, M. Lisker, L. Zimmermann, and M. Böhm, J. Opt. Soc. Am. B **31**, 2846 (2014).
10. H. Zhao, B. Kuyken, S. Clemmen, F. Leo, A. Subramanian, A. Dhakal, P. Helin, S. Severi, E. Brainis, G. Roelkens, and R. Baets, Opt. Lett. **40**, 2177 (2015).
11. J. P. Epping, T. Hellwig, M. Hoekman, R. Mateman, A. Leinse, R. G. Heideman, A. van Rees, P. J. van der Slot, C. J. Lee, C. Fallnich, and K.-J. Boller, Opt. Express **23**, 19596 (2015).
12. D. Carlson, D. Hickstein, A. Lind, J. Olson, R. Fox, R. Brown, A. Ludlow, Q. Li, D. Westly, H. Leopardi, T. Fortier, K. Srinivasan, S. Diddams, and S. Papp, "Photonic-chip supercontinuum with tailored spectra for precision frequency metrology," arXiv:1702.03269 (2017).
13. D. J. Jones, S. A. Diddams, J. K. Ranka, A. Stentz, R. S. Windeler, J. L. Hall, and S. T. Cundiff, Science **288**, 635 (2000).
14. A. S. Mayer, A. Klenner, A. R. Johnson, K. Luke, M. R. E. Lamont, Y. Okawachi, M. Lipson, A. L. Gaeta, and U. Keller, Opt. Express **23**, 15440 (2015).
15. A. Klenner, A. S. Mayer, A. R. Johnson, K. Luke, M. R. E. Lamont, Y. Okawachi, M. Lipson, A. L. Gaeta, and U. Keller, Opt. Express **24**, 11043 (2016).
16. I. Hartl, G. Imeshev, M. E. Fermann, C. Langrock, and M. M. Fejer, Opt. Express **13**, 6490 (2005).
17. A. Ishizawa, T. Nishikawa, S. Aozasa, A. Mori, O. Tadanaga, M. Asobe, and H. Nakano, Opt. Express **16**, 4706 (2008).
18. T. Jiang, A. Wang, G. Wang, W. Zhang, F. Niu, C. Li, and Z. Zhang, Opt. Express **22**, 1835 (2014).
19. K. Beha, D. C. Cole, P. Del'Haye, A. Coillet, S. A. Diddams, and S. B. Papp, Optica **4**, 406 (2017).
20. T. Herr, V. Brasch, J. D. Jost, C. Y. Wang, N. M. Kondratiev, M. L. Gorodetsky, and T. J. Kippenberg, Nat. Photonics **8**, 145 (2013).
21. J. Cardenas, C. B. Poitras, K. Luke, L.-W. Luo, P. A. Morton, and M. Lipson, IEEE Photon. Technol. Lett. **26**, 2380 (2014).
22. T. G. Tiecke, K. P. Nayak, J. D. Thompson, T. Peyronel, N. P. D. Leon, V. Vuletić, and M. D. Lukin, Optica **2**, 70 (2015).
23. S. Gröblacher, J. T. Hill, A. H. Safavi-Naeini, J. Chan, and O. Painter, Appl. Phys. Lett. **103**, 181104 (2013).
24. L. Chen, C. R. Doerr, Y.-K. Chen, and T.-Y. Liow, IEEE Photon. Technol. Lett. **22** 1744 (2010).
25. V. R. Almeida, R. R. Panepucci, and M. Lipson, Opt. Lett. **28**, 1302 (2003).
26. L. C. Sinclair, J.-D. Deschênes, L. Sonderhouse, W. C. Swann, I. H. Khader, E. Baumann, N. R. Newbury, and I. Coddington, Rev. Sci. Instrum. **86**, 081301 (2015).
27. Z. Zhang, C. Mou, Z. Yan, K. Zhou, L. Zhang, and S. Turitsyn, Opt. Express **21**, 28297 (2013).
28. X. Li, W. Zou, G. Yang, and J. Chen, IEEE Photon. Technol. Lett. **27**, 93 (2015).
29. M. A. G. Porcel, F. Schepers, J. P. Epping, T. Hellwig, M. Hoekman, R. G. Heideman, P. J. M. van der Slot, C. J. Lee, R. Schmidt, R. Bratschitsch, C. Fallnich, and K.-J. Boller, Opt. Express **25**, 1542 (2017).
30. J. M. Dudley, G. Genty, and S. Coen, Rev. Mod. Phys. **78**, 1135 (2006).
31. X. Guan, Y. Ding, and L. H. Frandsen, Opt. Lett. **40**, 3893 (2015).
32. A. B. Fallahkhair, K. S. Li, and T. E. Murphy, J. Lightwave Technol. **26**, 1423 (2008).